International Global Navigation Satellite Systems Association
IGNSS Symposium 2018

Colombo Theatres, Kensington Campus, UNSW Australia
7 – 9 February 2018

Compact multi-GNSS PPP corrections messages for transmission through a 250 bps channel

Ken Harima
School of Science / RMIT University / Australia
T: +61-3-99253775, E: ken.harima@rmit.edu.au
Suelynn Choy
School of Science / RMIT University / Australia
T: +61-3-99252650, E: suelynn.choy@rmit.edu.au
Chris Rizos
School of Civil and Environmental Engineering/ University of New South Wales / Australia
T: +61-2-93854205, E: suelynn.choy@rmit.edu.au

ABSTRACT

Precise Point Positioning (PPP) has been a target for a lot of research over the last few decades. The comparatively low infrastructure requirements and wide area applicability makes the system attractive as a nation-wide positioning system. Real-time corrections for PPP are now available through private and public entities, and have demonstrated the feasibility of sub-decimetre-level accuracy position and navigation using PPP. Delivery of these corrections through a satellite broadcast is an ideal fit for a precise position infrastructure. In addition, developments in multi-frequency PPP, multi-GNSS PPP and efforts to estimate ionospheric delays over wide areas has the potential to reduce convergence times and expand the applicability of PPP. However these improvements will require an increased amount of data to be transmitted to the user. Legacy SBAS channels are limited to 250 bps and often have only one satellite available as a transmitter. The present study explores the feasibility of delivering multi-frequency, multi-GNSS PPP systems using a 250 bps channel. Real-time streams for PPP were re-encoded into compact messages designed to fit into 250 bps channels used by current SBAS downlinks. Corrections based on CNES's CLK93 stream and JAXA's MDC1F streams were used base for the compact PPP messages. Corrections from the CLK93 stream occupied about 51% of the 250 bps channel capacity once compacted, while corrections from MDC1 occupied 52%. The original streams had an average data rate of 6.4 kbps (CLK93) and 22.4 kbps (MDC1). Real-time PPP solutions were computed using both the original real-time streams and the compacted PPP streams. For the MDC1 stream the horizontal accuracy after one hour of convergence was 4.28cm using the compact messages and 3.64cm using the original stream. For the CLK93 stream, horizontal accuracy was 3.69cm using the compact messages and 3.25cm using the original messages. Convergence times were similar, between 20 and 40 minutes, for the compact and original streams. In future versions, the remaining channel capacity on the 250 bps channel could be used to encode a regional ionosphere model to accelerate the PPP convergence.

KEYWORDS: PPP, multi-GNSS, SBAS channels.

1. INTRODUCTION

The increased interest in machine control is expected to expand the market for high accuracy GNSS positioning far beyond its legacy applications such as surveying. Implementation of Intelligent Transport Systems (ITS) will require GNSS augmentation systems of high accuracy and high reliability. As demands for these and other position-based services become widespread the demands on GNSS augmentation system infrastructure must be considered.

Most currently operating high accuracy positioning systems are based on differential techniques, such as the Real-Time-Kinematic (RTK) positioning technique, and variations thereof. These systems account for systematic errors in GNSS signals by calculating double-differences between the observations from the user receiver with those obtained from one or more nearby reference stations. While RTK can provide centimetre-level accuracy with convergence times of a few seconds, the requirement for reference station(s) near the user may make these systems unsuitable for deployment as infrastructure over wide areas. One alternative high accuracy positioning technique, known as Precise Point Positioning (PPP), has attracted research interest as it only requires a sparse network of global reference stations. PPP has already demonstrated its capability of delivering decimetre-level accuracy (Kouba, 2009; Zumberge et al., 1997), and few centimetre-level accuracy when ambiguity resolution is performed (Ge et al., 2007; Laurichesse et al., 2009).

PPP services only require the timely transmission of precise satellite orbits, clock offset corrections and GNSS measurement biases. A combination of PPP-based positioning and satellite-based delivery of the required products makes an attractive wide area positioning infrastructure. As such multiple PPP services are being planned or deployed worldwide both by private, e.g. Trimble's CenterPoint RTX (Trimble, 2017), and public agencies, e.g. Galileo's Commercial Service (Fernandez Hernandez, 2015). In the Asia-Pacific region, the Japanese Quasi-Zenith Satellite System (QZSS) is scheduled to start operations as a GNSS augmentation system in 2018. The QZSS will transmit a variety of GNSS augmentation messages, and a set of messages for real-time PPP based on the Multi-GNSS Advanced Demonstration tool for Orbit and Clock Analysis (MADOCA) software is under consideration (JAXA, 2017).

Recent research efforts are focused on reducing the long convergence time of PPP solutions in order to make it more suitable for practical applications. The modifications being proposed include the use of: multi-GNSS data, triple-frequency data, and ionospheric delay maps/models. While some these approaches show some promise, they often imply a significant increase in the amount of data to be transmitted to the user. If these corrections are to be transmitted through a satellite downlink complex data for an increasing number of satellites will need to be included in the limited bandwidth of the satellite downlink. The fact that satellite downlinks with frequencies around the L-band, which is the range of frequencies GNSS receivers are tuned to, are scarce and limited in bandwidth leads to the need to carefully assess what type of corrections can fit into these limited downlinks without incurring significant loss of PPP performance.

The research presented in this paper describes how GNSS corrections for PPP-AR can be compacted to fit into a 212 bps stream. In similar work (Aubault-Roudier, 2016) ephemeris for 20 satellites were transmitted using part of a satellite downlink (125 bps) with a moderate degradation in performance. We propose an encoding scheme aimed at transmitting corrections for 50 satellites or more without significant loss of performance in PPP solutions.

2. PRECISE POINT POSITIONING

There are many algorithms that can be described as PPP algorithms. The algorithms presented here are separated according to the type of information needed. First the basic real-valued ambiguity PPP requires only satellite orbit and clock offset corrections. Ambiguity resolved PPP (referred to as PPP-AR in this document) requires the standard corrections for PPP as well as carrier phase biases, code

biases, or a combination of both. Finally ionosphere-assisted PPP (PPP-RTK in this document) requires ionospheric corrections in addition to the corrections for PPP-AR.

PPP is based on the robust modelling and compensation of errors in the GNSS measurements (Kouba, 2009). The PPP algorithms targeted by the SBAS messages are based on the following GNSS measurement model:

$$P_i^S = \rho^S + cdt^S + \frac{\lambda_i^2}{\lambda_1^2} I_1^S + B_i^S - B_i + \epsilon_i^S \quad (1)$$

$$L_i^S = \rho^S + cdt^S - \frac{\lambda_i^2}{\lambda_1^2} I_1^S + \lambda_i N_i^S + b_i^S - b_i + d\varphi_i^S + \varepsilon_i^S \quad (2)$$

where P_i^S and L_i^S are the pseudorange and carrier phase measurements and ρ^S is the geometric component of the measurements, this includes the distance between the satellite and receiver position, the receiver clock offset and tropospheric delays, the receiver position is ultimately calculated from these values. The speed of light *c* and the carrier wavelength λ_i are known values. Phase delays such as phase windup and antenna effects $d\varphi_i^S$ are estimated from empirical models. The carrier phase ambiguities N_i^S are estimated alongside the geometry components. The satellite position and clock offset dt^S are corrections transmitted to the end user and thus needs to be included in the PPP correction messages. How to handle the satellite code biases B_i^S, satellite phase biases b_i^S and the ionospheric delays I_1^S is what distinguishes the different PPP algorithms. The receiver biases have been removed from the equations for simplicity, as they are generally assimilated by the receiver clock offset, ionospheric delay estimate and real-valued ambiguities.

The most basic form of correction messages for PPP only contains the satellite position and the satellite clock offset. It is understood here that the satellite clock offset refers to the ionosphere-free combination of L1 and L2 pseudoranges, and the solution is meant to be used for dual-frequency measurements. When corrected for the satellite clock offset the measurement models in (1) and (2) can be expressed as:

$$P_i^S - cdt^S = \rho^S + \frac{\lambda_i^2}{\lambda_1^2} I'^S_1 + \epsilon_i^S \quad (3)$$

$$L_i^S - cdt^S - d\varphi_i^S = \rho^S - \frac{\lambda_i^2}{\lambda_1^2} I'^S_1 + \left[\lambda_i N_i^S + b_i^S + \frac{\lambda_i^2}{\lambda_2^2 - \lambda_1^2}\left(B_2^S - B_1^S\right)\right] + \varepsilon_i^S \quad (4)$$

where

$$I'^S_1 = I_1^S + \frac{\lambda_1^2}{\lambda_2^2 - \lambda_1^2}\left(B_2^S - B_1^S\right). \quad (5)$$

In this case the receiver position, receiver clock offset, tropospheric delay and ionospheric delay estimated alongside real-valued "floating ambiguities" corresponding to:

$$A_i^S = \lambda_i N_i^S + b_i^S + \frac{\lambda_i^2}{\lambda_2^2 - \lambda_1^2}\left(B_2^S - B_1^S\right) \quad (6)$$

The first variants of the PPP algorithm (Zumberge, 1997) used the ionosphere-free combination to eliminate the effect of ionospheric delay instead of estimating it as a parameter, and in this case the measurement models, corrected for satellite clock offset, becomes:

$$P_{IF}^S - cdt^S = \rho^S + \epsilon_{IF}^S \quad (7)$$

$$L_{IF}^S - cdt^S - d\varphi_{IF}^S = \rho^S + \left[\frac{\lambda_1\lambda_2}{\lambda_2^2 - \lambda_1^2}\left(\lambda_2 N_1^S - \lambda_1 N_2^S\right) + \frac{\lambda_2^2}{\lambda_2^2 - \lambda_1^2} b_1^S - \frac{\lambda_1^2}{\lambda_2^2 - \lambda_1^2} b_2^S\right] + \varepsilon_{IF}^S \quad (8)$$

where P_{IF}^S and L_{IF}^S are the ionosphere-free combination of pseudorange and carrier phase measurements, $d\varphi_{IF}^S$ is the ionosphere-free combination of modelled phase errors, and the "floating ambiguity" becomes:

$$A_{IF}^S = \frac{\lambda_1\lambda_2}{\lambda_2^2 - \lambda_1^2}\left(\lambda_2 N_1^S - \lambda_1 N_2^S\right) + \frac{\lambda_2^2}{\lambda_2^2 - \lambda_1^2} b_1^S - \frac{\lambda_1^2}{\lambda_2^2 - \lambda_1^2} b_2^S \quad (9)$$

2.1. Ambiguity resolution in PPP

In order to improve convergence time and position accuracy, modern PPP algorithms attempt to isolate and resolve the integer ambiguities N_i^S (Ge, 2008; Larichesse, 2009). The approach taken by

the RTCM standard is to transmit both the satellite hardware bias for pseudorange and carrier phase measurements to the end user. The GNSS measurement, when corrected for code and phase biases can be modelled as:

$$P_i^S - \boldsymbol{cdt^S} - \boldsymbol{B_i^S} = \rho^S + \frac{\lambda_i^2}{\lambda_1^2} I_1^S + \epsilon_i^S \tag{10}$$

$$L_i^S - \boldsymbol{cdt^S} - \boldsymbol{b_i^S} - d\varphi_i^S = \rho^S - \frac{\lambda_i^2}{\lambda_1^2} I_1^S + \lambda_i N_i^S + \varepsilon_i^S \tag{11}$$

from which the end user can estimate the receiver position, receiver clock offset, zenith tropospheric delay, the unbiased ionospheric delay and the carrier phase ambiguity. If no ionospheric corrections are transmitted to the user, it is not necessary to transmit both the phase biases and code biases.

If the code biases are not transmitted, the pseudorange measurement model will be the same as equation (3). This means the user is going to estimate the biased ionospheric delay I'^S_1 shown in equation (5). In order for this to be the case, the phase biases need to be adapted so that the carrier phase measurement produces the same biased ionospheric correction. If the satellite clock corresponds to the ionosphere-free combination of pseudorange measurements and thus $\frac{\lambda_2^2}{\lambda_2^2-\lambda_1^2} B_1^S - \frac{\lambda_1^2}{\lambda_2^2-\lambda_1^2} B_2^S = 0$, then the modified phase bias can simply be $b'^S_i = b_i^S + B_i^S$. In a more general case, where the corrections need to be transformed from a set of corrections for which $\frac{\lambda_2^2}{\lambda_2^2-\lambda_1^2} B_1^S - \frac{\lambda_1^2}{\lambda_2^2-\lambda_1^2} B_2^S \neq 0$, then the clock correction and phase biases need to be defined as:

$$cdt'^S = cdt^S + \frac{\lambda_2^2}{\lambda_2^2-\lambda_1^2} B_1^S - \frac{\lambda_1^2}{\lambda_2^2-\lambda_1^2} B_2^S \tag{12}$$

$$b'^S_i = b_i^S - \frac{\lambda_i^2+\lambda_2^2}{\lambda_2^2-\lambda_1^2} B_1^S + \frac{\lambda_i^2+\lambda_1^2}{\lambda_2^2-\lambda_1^2} B_2^S \tag{13}$$

in (13) dt^S, b_i^S and B_i^S are assumed to be a set of corrections capable of isolating the integer ambiguity and dt^S is a satellite clock offset that does not correspond to the ionosphere-free combination of L1 and L2 pseudorange measurements. Using the set of corrections in (13) and (14) the measurement models in (1) and (2) become:

$$P_i^S - \boldsymbol{cdt'^S} = \rho^S + \frac{\lambda_i^2}{\lambda_1^2} I'^S_1 + \epsilon_i^S \tag{14}$$

$$L_i^S - \boldsymbol{cdt'^S} - \boldsymbol{b'^S_i} - d\varphi_i^S = \rho^S - \frac{\lambda_i^2}{\lambda_1^2} I'^S_1 + \lambda_i N_i^S + \varepsilon_i^S \tag{15}$$

In PPP algorithms that use the ionosphere-free combination, the Melbourne-Wubenna combination is added for the purposes of ambiguity resolution:

$$P_{IF}^S - cdt^S - B_{IF}^S = \rho^S + \epsilon_{IF}^S \tag{16}$$

$$L_{IF}^S - cdt^S - b_{IF}^S - d\varphi_{IF}^S = \rho^S + \frac{\lambda_1\lambda_2}{\lambda_1+\lambda_2} N_1^S + \frac{\lambda_2}{\lambda_2^2-\lambda_1^2}\left(N_1^S - N_2^S\right) + \varepsilon_{IF}^S \tag{17}$$

$$P_{MW}^S - d\varphi_{MW}^S - B_{MW}^S - b_{MW}^S = \frac{\lambda_1\lambda_2}{\lambda_1-\lambda_2}\left(N_1^S - N_2^S\right) + \epsilon_{IF}^S + \varepsilon_{MW}^S \tag{18}$$

When corrected for the default PPP-AR corrections, both code and phase biases, the Melbourne–Wubenna combination isolates the $N_1^S - N_2^S$ ambiguities. Once this ambiguity is solved, N_1^S can be estimated along with receiver positions and other parameters using (17) and (18). It can be shown that in this particular case, the modified biases in equations (12) and (13) leads to the same corrections as the default correction for all combinations:

$$P_{IF}^S - \boldsymbol{cdt'^S} = P_{IF}^S - cdt^S - \boldsymbol{B_{IF}^S} \tag{19}$$

$$L_{IF}^S - \boldsymbol{cdt'^S} - \boldsymbol{b'^S_{IF}} = L_{IF}^S - \boldsymbol{cdt^S} - \boldsymbol{b_{IF}^S} \tag{20}$$

$$P_{MW}^S - \boldsymbol{b'^S_{MW}} = P_{MW}^S - \boldsymbol{b_{MW}^S} - \boldsymbol{B_{MW}^S} \tag{21}$$

Although ignored above for simplicity, the receiver biases, both in pseudorange and phase measurments need to be taken into account when solving ambiguities. In our study we adopt the algorithm proposed by Ge (Ge, 2008). In this method, satellite single-differenced ambiguities are solved instead of the absolute ones. Once the single difference observations are solved, the difference between single solved and floating ambiguities ar applied as an extra measurement/ innovation to refine the PPP solution.

2.2. Ionospheric corrections in PPP

The inclusion of ionospheric delay corrections is known to accelerate the otherwise long convergence times associated with PPP solutions. Because ionosphere corrections are local in nature, these corrections will take the form of maps over the region of coverage.

Most of the PPP-RTK solutions presented in the literature (e.g. Li, 2014) use Slant Total Electron Content (STEC) maps in order to represent the state of the ionosphere over the region of coverage. In terms of PPP message simplicity, the advantage of using STEC is that it simplifies the representation of the ionosphere and avoids the need of separating satellite biases from the ionosphere. For these types of ionosphere corrections, maps of biased ionospheric delays I'^{S}_{1} need to be added to the PPP solutions. The main disadvantage of STEC, or any satellite-specific ionospheric delay corrections, is that one such map is required for each satellite, and for a multi-GNSS scenario this becomes impractical as close to 140 satellites are expected to be soon operational, including GPS, GLONASS, Galileo, BeiDou and QZSS satellites.

Efforts to estimate an integrated ionosphere, capable of representing all satellites in one map, have met with mixed success (Juan, 2012; Zhang, 2013; Banville, 2014; Rovira-Garcia, 2015). However, it can be expected that these maps will be available in the future. It may be possible to transmit these kinds of maps through satellite downlinks once they become accurate enough for PPP-RTK. This type of ionospheric delay correction will correspond to unbiased ionosphere I^{S}_{1} and thus both code and phase biases for each satellite need to be transmitted alongside the ionospheric delay maps.

Table 1 shows the corrections required for the PPP solutions discussed above. The solutions discussed are applicable mostly for dual-frequency PPP. For triple-frequency PPP an additional code and phase bias corresponding to the third frequency need to be added. The PPP messages tested in this research correspond to messages for dual-frequency PPP-AR, which includes satellite orbits, satellite clock offsets and modified phase biases for two signals.

Channel	Ephemeris	Phase bias	Code bias	Ionosphere
PPP	1 x Nsat	-	-	-
PPP-AR	1 x Nsat	2 x Nsat	-	-
PPP-RTK (STEC)	1 x Nsat	2 x Nsat	-	Nsat
PPP-RTK (Integrated)	1 x Nsat	2 x Nsat	2 x Nsat	1

Table 1. Corrections for different PPP services

3. SBAS CHANNEL AND COMPACT PPP

As mentioned in previous sections PPP requires the timely delivery of the GNSS corrections listed in Table 1. The most suitable means of doing this over a wide area is to use a satellite communications channel. Moreover, to minimise the additional hardware required by the end user, the satellite channel should have a signal carrier in or close to the L-band signals currently used by GNSS. However, the satellite communications channels in this band are scarce and limited in bandwidth.

Traditionally signals in this band dedicated to augmenting the performance of GNSS signals have been designed to accommodate the RTCA-defined Satellite Based Augmentation System (SBAS) messages. Examples of these SBAS systems are: the Wide Area Augmentation System (WAAS) in North America, the European Geostationary Navigation Overlay System (EGNOS) in Europe, the Multi-Functional Satellite Augmentation System (MSAS) in Japan, and the GPS and GEO Augmented Navigation (GAGAN) system in India.

These traditional SBAS messages consist of a stream of 250 bit frames transmitted every second. The frames include an 8 bit preamble, 6 bits indicating the type of message and 24 bits of parity check,

leaving 212 bps of effective data rate. Other types of SBAS currently under development are listed in Table 2 along with their effective data rates.

Channel	Carrier freq.	Total data rate	Effective data rate
L1 SBAS	1575.42 MHz	250 bps	212 bps
L5 SBAS	1176.45 MHz	250 bps	216 bps
Galileo CS	1278.75 MHz	500 bps	448 bps
QZSS L6	1278.75 MHz	2000 bps	1695 bps

Table 2. Satellite channels for GNSS augmentation

The L5 SBAS listed in Table 2 is also referred to as Dual-Frequency Multi-Constellation (DFMC) SBAS, or SBAS 2.0, and is designed for dual-frequency receivers. The use of dual-frequency dispenses with the need for the accurate ionosphere maps which is characteristic of single-frequency receivers. This in turn allows space for a larger number of corrections for satellites. The DFMC messages have also a higher resolution than legacy SBAS messages, which makes than suitable for sub-metre accuracy pseudorange-based positioning, but it falls short of supporting PPP.

Channels intended for PPP include the Galileo Commercial service (Fernandez-Hernandez, 2015), and the QZSS L6 channel. Both of these signals boast higher data rates than traditional SBAS services, in order to accommodate the data rates that are required for PPP. Both have demonstrated, in preliminary tests, to be capable of delivering decimetre to centimetre-level accuracy in positioning. In this paper we will design and test messages for multi-GNSS PPP that can be transmitted using the 212bps SBAS channels. Accommodating similar messages in higher data rate channels should be straight forward.

3.1. Compact messages for PPP

In order to support PPP-AR services the user needs to receive enough information to calculate the precise satellite position, precise satellite clock offset and the modified satellite phase biases in (13). Of these corrections, the orbit and phase biases are known to be stable or predictable for periods of time spanning a few hours. The satellite clock offset on the other hand is much more difficult to predict and thus are often updated every few seconds.

The general structure for the proposed compact PPP messages is shown in Figure 1. The message design draws inspiration from the RTCM message format and the RTCA standard. The message numbers that are used are arbitrary selected as 52 to 56. Message type 52 is the equivalent of the PRN mask message for the RTCA standard messages, and includes a time tag which contains information on the time of week with a resolution of 30 seconds, and a PRN mask which tells the end user which satellites have corrections included in the following messages. For the tests performed in this paper these messages were updated every 2 minutes. The ephemeris and bias data are transmitted in the order established by the PRN mask during the validity of the satellite mask, indicated by the IOD field at the beginning of each frame.

Similar to the RTCA messages, the satellite clock offset is defined using fast and slow corrections. Messages type 53 to 56 contain a different mix of “slow data” and “fast data” fields as shown in Figure 1. For the tests discussed in this paper, the slow data is used to transmit:

- Corrections to satellite position every 2 minutes
- Phase bias to two signals every 2 minutes

Corrections to satellite position consist of radial, along-track and cross-track corrections to the satellite position calculated using the navigation messages broadcast by the GNSS satellite, similar to the RTCM 3.2 format. Phase biases correspond to the modified phase bias in (13) for the L1C/A and L2P signals in GPS, L1C and L2C signals in GLONASS, E1 and E5a signals in Galileo, B1 and B2 signals in BeiDou, and L1/CA and L2C in QZSS.

The fast data contains a satellite number and either an alert flag or a correction to the last satellite clock offset sent in a slow data field. In the end user receives a fast data field containing a correction,

this correction should be added to the last satellite clock offset transmitted in a slow data field. If the end user identifies a fast data field with an alert flag, data for the corresponding satellite has become unreliable and should be ignored.

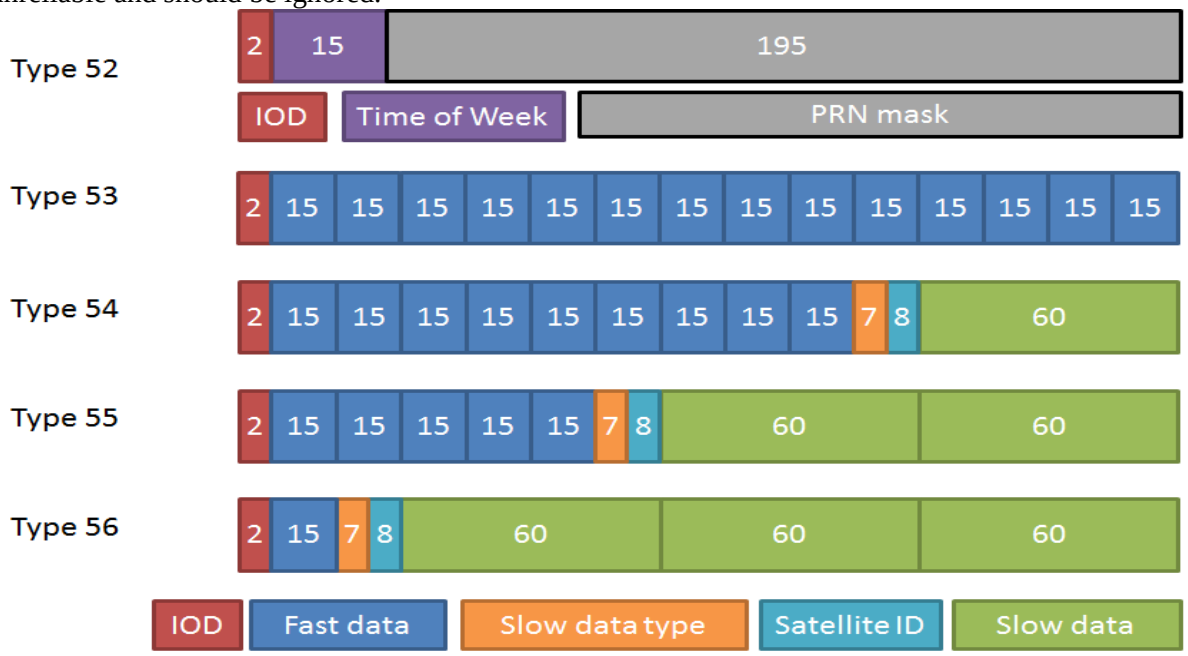

Figure 1. Structure of compact messages for PPP using 212 bps

The number of fast data fields (and thus message types) changes to allow the transmission of all necessary fast corrections. It is also to note that in the event of a IODE change on the encoder side the difference between the broadcast ephemeris are taken into account to decide whether the alert flag is sent or not. All radial and clock corrections have a resolution of 5mm, along-track and cross-track corrections have resolution of 2cm. The phase bias has a resolution of 1/32 cycles and a dynamic range of ±2 cycles. This means that the user needs to be aware of the possibility of a 2 cycle jump in these corrections and compensate for it accordingly.

3.2. Effect of data compression on correction accuracy

In order to evaluate the feasibility of using the compact messages for PPP, correction messages for two real-time streams were re-packaged as 250 bps messages and used to obtain real-time PPP solutions. The two streams used for these tests where the CLK93 stream produced by the French Space Agency CNES using its PPP-Wizard software, and the MDC1F stream produced by the Japanese Aerospace Exploration Agency JAXA using its MADOCA software.

Figure 2 shows a diagram of the tests to investigate the compact PPP messages. The RTCM 3.2 encoded corrections were converted in real-time to 250 bps messages and broadcast using an NTRIP caster. On the user end the compact messages were converted back to RTCM-formatted messages and used to calculate PPP solutions. We will call the messages converted back to RTCM at the user end "recovered messages" in this paper.

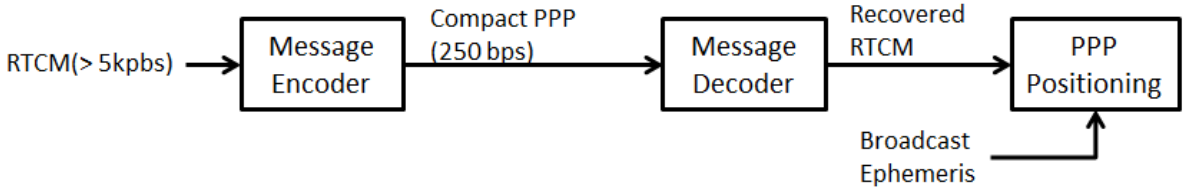

Figure 2. Set-up for real-time tests of compact messages for PPP

First we evaluated the accuracy of the satellite orbit and clock offset corrections contained in the PPP messages both before and after transmission. The final multi-GNSS ephemeris from CODE (Prange, 2017) was used as reference to evaluate the accuracy of the real-time products. It is to be noted that the real-time and CODE products are expected to have different system clocks as well as a different network pivot. This means that two components of the errors need to be discarded from the satellite clock offset estimates, first a common component among the satellites of a constellation representing the difference in system clock, secondly a constant bias in each satellite which represents the difference between network pivots.

The CLK93 stream contains orbit corrections, clock corrections, code bias and phase biases for GPS, GLONASS Galileo and BeiDou satellites. Corrections for BeiDou satellites are not yet accurate enough to be useful in PPP and are sometimes absent. The total number of satellites for which corrections are included in the CLK93 stream varies from 69 to 79 depending on how many BeiDou satellites are included. The accuracy of the orbits, clock and range at the ALIC station for the recovered stream is shown in Figure 3. The bars represent, from left to right, radial (dark blue), along-track (medium blue), cross-track (light blue) and clock errors (orange) as well as the range difference at the ALIC station (yellow).

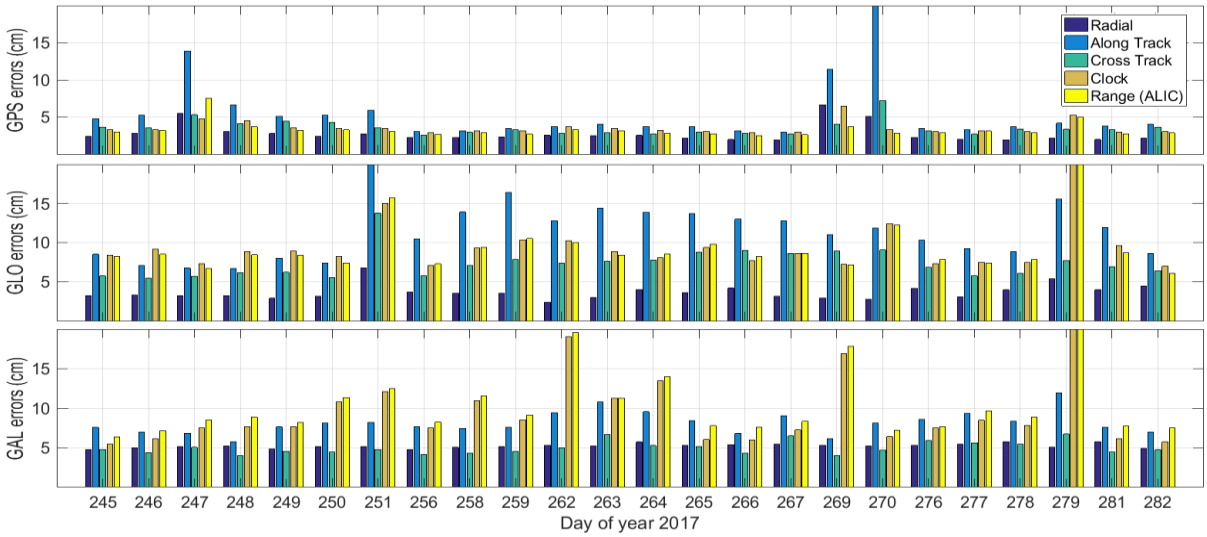

Figure 3. Orbit and clock errors for compact messages based on PPP-Wizard. Bars represent radial (dark blue), along-track (blue), cross-track (light blue), clock offset errors (orange) as well as the range difference at the ALIC station (yellow)

The values shown in Figure 3 correspond to the average of errors for the 24 days between September 2nd and October 10th 2017 were evaluated. Network outages as well as maintenance on the IGS NTRIP caster prevented us from obtaining results for all days. The RMS values for the orbit and range differences are presented in Table 3. For GPS satellites, the CLK93 messages and its recovered version have a range difference of around 3cm with very few differences noticeable between the accuracy before and after the conversion to 250 bps. For the total range there is an accuracy degradation of about 5mm. The range accuracy of GLONASS and Galileo is at the decimetre-level, mostly due to clock errors. For GLONASS there is an accuracy degradation of a few mm in both orbit and range between the original and recovered messages, however given the total range accuracy of 10cm, 3 to 5mm are not expected to lead to significant differences.

The MDC1F stream contains satellite orbit corrections, satellite clock offset corrections, code biases and phase biases for GPS, GLONASS and QZSS satellites. With the exception of DOY 248, for which there was only an average of 38 satellites, the number of satellites for which corrections are transmitted is between 52 and 56. One of the main differences between this stream and the IGS real-time streams is that both orbit and clock corrections are updated each second. In contrast to corrections the CLK93 stream is updated every 5 second. For this reason the data rate for the original stream is

22.4 kbps as opposed to 6.4 kbps for the case of CLK93. The accuracy of orbits, clock and range at the ALIC station for the recovered stream is shown in Figure 4.

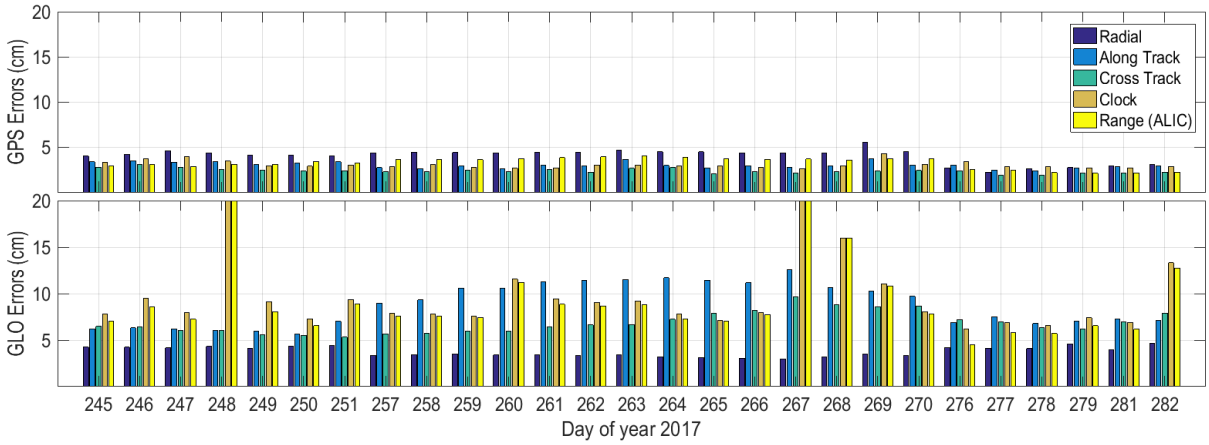

Figure 4. Satellite orbit and clock offset errors for compact messages based on MADOCA

As with Figure 3, the bars represent radial (dark blue), along-track (medium blue), cross-track (light blue) and clock offset errors (orange), as well as the range difference at the ALIC station (yellow). At first glance the accuracy of the GPS products seems to be better than those of CLK93. However the advantage of MDC1F is mainly with respect to the along-track and cross-track components, while the errors in radial component are significantly larger, leading to an orbit accuracy of around 4cm as shown in Table 3. The range accuracy is comparable to CLK93 for both GPS and GLONASS. In this case the range accuracy degradation is about 6-7mm for GPS, 2mm in GLONASS, and the effect of the GLONASS corrections should not be noticeable (as it only represents 2% of accuracy degradation). The difference in GPS products amount to a 20% increase in range errors which should be the main source of difference in PPP performance.

	CLK93 RTCM	CLK93 Compact	MDC1F RTCM	MDC1F Compact
GPS Orb	3.18 cm	3.17 cm	4.03 cm	4.12 cm
GPS Range	2.95 cm	3.41 cm	3.27 cm	3.92 cm
GLO Orb	3.79 cm	4.25 cm	4.06 cm	4.23 cm
GLO Range	9.99 cm	10.34 cm	10.28 cm	10.45 cm
GAL Orb	5.37 cm	5.32 cm	-	-
GAL Range	11.81 cm	11.56 cm	-	-
Data rate	6.4 kbps	250 bps	22.4 kbps	250 bps

Table 3. Orbit and range error for RTCM and compact messages for PPP

It is to be note here that the PPP product accuracy is evaluated at the time of the CODE final products which have an update time of 5 minutes. The real-time streams are updated every 1 or 5 seconds which means that the maximum age of ephemeris is 4 seconds. The compact PPP on the other hand updates every 2 minutes, and the orbit and slow clocks are updated during the first 30 seconds of that period. This means that half of the orbit products have an age of correction of 30 seconds to 1 minute while the other half have an age of 1.5 to 2 minutes.

4. PPP SOLUTIONS USING COMPACT PPP

PPP solutions were calculated in real-time using both the RTCM stream directly and the corrections recovered from the 250 bps messages. Real-time observations from the ALIC CORS were used to calculate simulated kinematic PPP solutions for a rover receiver. Although the ALIC receiver is connected to a static antenna (ANTEX code LEIAR25.R3) at approximate coordinates 23˚ 40’ 12” S, 133˚ 53’ 08”E, the processing software was set to assume a moving antenna. A modified version of the RTKLIB (Takasu, 2009) application RTKNAVI was used to calculate the PPP solutions.

The algorithm in the RTKLIB software uses the ionospheric-free combination in (7) and (8) to calculate PPP solutions with real-valued ambiguities. This software was modified to use the Melbourne-Wubenna combination in (18) to isolate the ambiguities. The signal biases generated by the MADOCA software as well as those generated for Galileo satellites by the PPP-Wizard software were found to be inadequate for ambiguity resolution. For this reason ambiguity resolution was performed only on GPS satellites when using PPP-Wizard corrections. The modified lambda method (Chang, 2009) was used to solve for the ambiguities. In order to evaluate the solution convergence as well as the steady state accuracy, the solutions were set to reset every 3 hours. The ephemeris range errors were set to 3cm for GPS and 10cm for both GLONASS and Galileo.

The MADOCA based solutions were calculated from September 2nd to September 21st (DOY 264) 2017. The QZSS corrections were found to be unsuitable for PPP (errors at the metre-level with respect to the CODE values) thus the MADOCA based solutions used only GPS and GLONASS satellites. Although signal outages prevented us from obtaining all possible solutions, a total of 130 solutions were obtained.

PPP-Wizard based solutions were calculated from September 22nd to October 10th 2017. Technical difficulties with the NTRIP caster used prevented us from perform concurrent test with the MDC1F. In this case BeiDou corrections were found to be unsuitable for PPP thus the PPP-Wizard based solutions use only GPS, GLONASS and Galileo measurements. Multiple instances were noted in which the Galileo corrections from CLK93 corresponded to the broadcast ephemeris values that were yet to be included in the IGS real-time stream. In these cases the PPP solution was not able to use the Galileo satellites for a few minutes and thus there was a reset of the ambiguity estimation corresponding to those satellites. It is thus suspected that a large number of solutions do not benefit from Galileo satellite observations. A total of 102 solutions were obtained using the PPP-Wizard based corrections.

4.1. PPP solutions based on CNES's PPP-Wizard

As mentioned above, corrections from real-time streams for PPP were encoded into the compact PPP messages shown in Figure 1. In the case of the CLK93 stream the contents of the compact PPP messages are described in Table 4. The first column of Table 4 shows the type of data, high rate clock represents the fast data fields used for clock offset corrections; ephemeris and signal bias represent the slow data fields used to transmit these quantities; the free fields represent unused slow data fields; the null messages are messages that are transmitted when there is no data to transmit; and the overhead represent all bits not included on the fields above. The last column is the data size occupied by each type of data with respect to the number of satellites included in the corrections, and is calculated by linear fitting daily averages.

	# of fields/ 2 min	Data rate	Occupancy	Rate vs Nsat
Overhead	-	46.0 bps	18.4%	7.26 + 0.27 x Nsat
High rate clock	374.6	46.8 bps	18.7%	13.88 + 0.44 x Nsat
Ephemeris	74.4	37.2 bps	14.9%	0.5 x Nsat
Signal bias	20.1	10.1 bps	4.0%	0.125 x Nsat
Free fields	14.6	7.3 bps	2.9%	3.05 + 0.06 x Nsat
Null messages	58.1	102.6 bps	41.0%	191.1 – 1.19 x Nsat

Table 4. Channel occupancy for PPP-Wizard based compact PPP messages

In the case of CLK93, the update rate of this stream's clock correction is 5 seconds, which means the fast data comes in a burst every 5 seconds. For the times where this happens, a messages type 53 or 54, consisting mostly of fast clock corrections, is transmitted. Together these two constitute about 20.6% of message types. For the remaining 80% of the time, there are few clocks to update thus message 56, when there is slow data to transmit, or the null message is transmitted. As shown in Table 4, 58.1 of the 120 messages transmitted every 2 minutes were null messages. The data section of these messages along with the space left in the free fields corresponds to 41% of the channel data capacity. Given that the average number of satellites encoded in the compact messages was 74.4 over the 24 days, this implies that the channel has a capacity for approximately 126 satellites.

The average number of satellites encoded in the compact messages was 74.4 over the 24 days the data was collected. The number of clock updates performed during that time was on average 74.4 + 374.6 every 2 minutes, which is equivalent to a per satellite update rate of 19.9 seconds.

A sample of PPP solutions, calculated on September 22nd 2017 between 9 am and 12 pm UTC can be seen in Figure 6. There is a 2 minute and 10 second difference in the time to achieve the first ambiguity-fixed solution. Since the stochastic model is the same for both solutions, this difference is presumably due to differences in the ratio tests used to validate the ambiguities, which in turn will come from differences in the real-value estimates of GPS ambiguities. It can also be seen that the probability of incorrectly fixing an ambiguity is higher at early stages of convergence. Once the ambiguities have been solved for correctly the differences between solutions are below the millimetre-level for horizontal position, and less than a few centimetres in the vertical component.

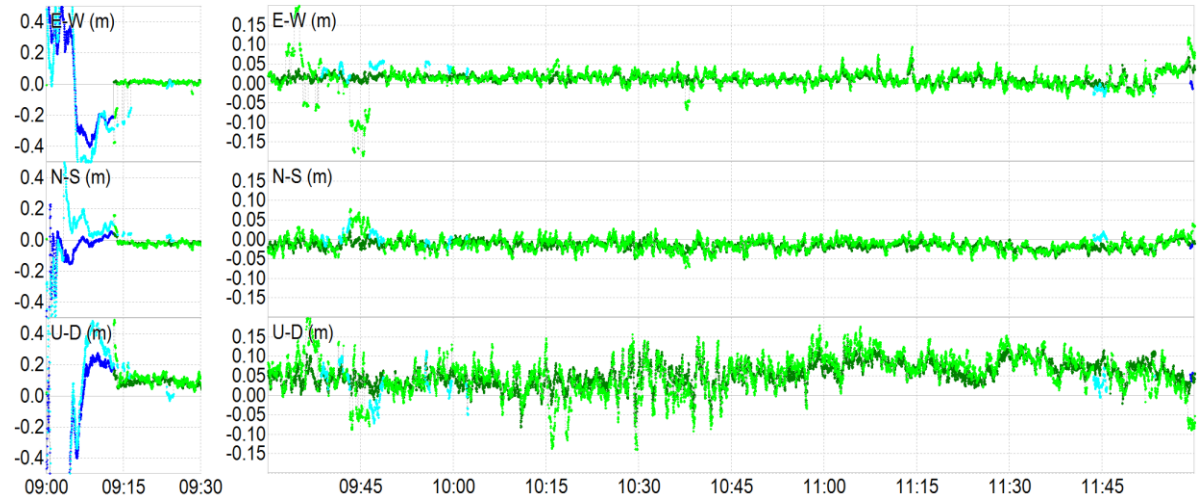

Figure 6. Difference between known positions and PPP solutions using original (dark blue and green) and recovered (light blue and green) messages. Solutions are based on observables from the ALIC station between 09:00 to 12:00 UTC, September 22, 2017. Blue dots represent solutions with float ambiguities while green dots represent solutions with fixed ambiguities.

The average performance of all 103 PPP-Wizard based PPP solutions are shown in Figure 7 and Table 5. Figure 7 was obtained by calculating the RMS difference between PPP solutions and the CORS known position at different convergence times. The first point corresponds to samples between 0 and 10 seconds since the start of the processing, the second point to samples between 10 and 20 seconds, and so on.

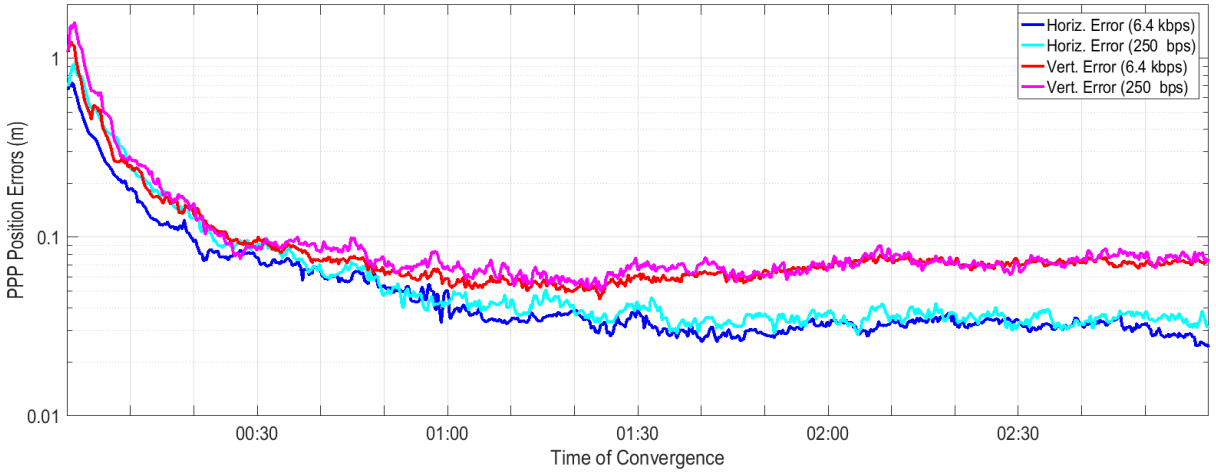

Figure 7. RMSE of horizontal (blue) and vertical (red) errors using original (dark) and recovered (light) messages. PPP solutions calculated using CLK93 between Sep. 22nd and Oct.10th 2017

In Figure 7, the blue lines correspond to horizontal position errors, the dark blue line to position using the original RTCM messages, and the light blue line to solutions using corrections recovered from compact messages. The red and pink lines correspond to vertical position errors obtained using the original and recovered streams respectively.

Table 5 shows an accuracy degradation of approximately 4mm in both the horizontal and vertical components, which represents a 13% increase for the horizontal component and a 6% increase in the vertical accuracy. The differences in convergence times are 16% for the horizontal components and 30% for the vertical component, although as it can be seen in Figure 7, this parameter had a large variation. A small difference in one of the solutions could push the convergence time for vertical solutions to 30 minutes or more in solutions using the original CLK93 products.

	CLK93 original	**CLK93 recovered**
Horizontal accuracy <10cm	19 min 40 sec	23 min 00 sec
Vertical accuracy <10cm	25 min 20 sec	36 min 20 sec
Horizontal accuracy after 1 hour	3.25cm	3.69cm
Vertical accuracy after 1 hour	6.57cm	6.95cm

Table 5. PPP performance using direct and recovered messages

As it can be seen in Figure 7 the two solutions are comparable, with no significant differences between solutions obtained from the original stream and the recovered stream. Although the PPP solution using the original stream is statistically better than the PPP solution using the recovered products, both have centimetre level horizontal accuracy and 10 cm vertical accuracy.

4.2. PPP messages based on JAXA's MADOCA

The contents of the compact PPP messages derived from the MDC1F stream is shown in Table 6. As a comparison with Table 4 will show, the data distribution was quite different for these messages. Since the MDC1F stream has an update rate of 1 second there is always new clock data that can potentially be transmitted. Because of this, the most common message was type 55 (transmitted when there is more than 1 but less than 6 satellite clocks to upgrade) corresponding to 56.8% of the messages, instead of the null message which only correspond to 12%.

	# of fields/ 2 min	**Data rate**	**Occupancy**	**Rate vs Nsat**
Overhead	-	54.6 bps	21.8%	47.4 + 0.15 x Nsat
High rate clock	429.5	53.7 bps	21.5%	20.42 + 0.68 x Nsat
Ephemeris	49.4	24.7 bps	9.9%	0.5 x Nsat
Signal bias	13.5	6.7 bps	2.7%	0.125 x Nsat
Free fields	169.8	84.9 bps	34.0%	77.58 + 0.16 x Nsat
Null messages	14.4	25.4 bps	10.2%	101.9 – 1.57 x Nsat

Table 6. Channel occupancy for MADOCA based compact PPP messages

Since messages 52, 53 and the null message represent about 13.1% of the total, 86.9% of messages had slow data fields, 73% of these remaining unfilled as there was no ephemeris or bias data to transmit. This means that the free space for MDC1F based compact messages was mainly located in the free fields. The combination of this and the space left in null messages correspond to about 52% of the channel capacity. Given that the average number of satellites for which there were corrections in the message was 49.4, the compact message will have a capacity for approximately 102 satellites. The difference in the maximum number of supported satellites comes from the effective clock rate. The number of fields that update clock correction was 479 for 49.4 satellites, which is equivalent to an update rate of 12.4 seconds, a significant reduction from an update rate of 1Hz but still a 50% faster rate than for CLK93.

A sample of PPP solutions, calculated on September 1st 2017, between 9 am and 12 pm UTC can be

seen in Figure 8. As with the CLK93 stream, the two solutions are of comparable accuracy. In this case since ambiguity resolution is not attempted, the differences between real-valued ambiguities produce a persistent difference between position solutions. These differences are accumulated from the slight differences between ephemeris, the differences can be expected to average to zero over long periods of time. In the case of the solutions in Figure 8 those differences can be of up to 5cm even after an hour of convergence, as seen in the E-W component between 10:00 and 10:15. Once the ambiguities have been estimated correctly the differences between solutions are below a few centimetres.

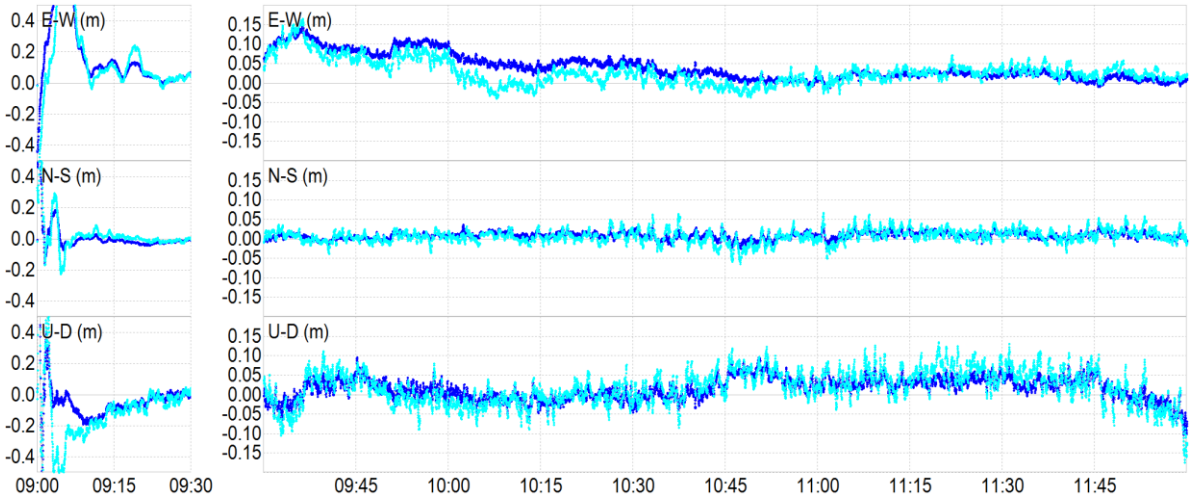

Figure 8. Difference between known positions and PPP solutions using (dark blue) and recovered (light blue) messages. Solutions are based on observables from the ALIC station between 09:00 to 12:00 UTC, Sep. 1st 2017.

The average performance of all 130 MADOCA based PPP solutions are shown in Figure 9 and Table 7. The RMSE values in Figure 9 were obtained in the same way as for Figure 7, and the solutions are represented by the same colours. The dark blue line represent horizontal errors of the solution obtained using the original MDC1F messages, while the red line represents vertical errors for the same solutions. The position errors for PPP using recovered RTCM messages are represented by the light blue (horizontal) and pink lines (vertical).

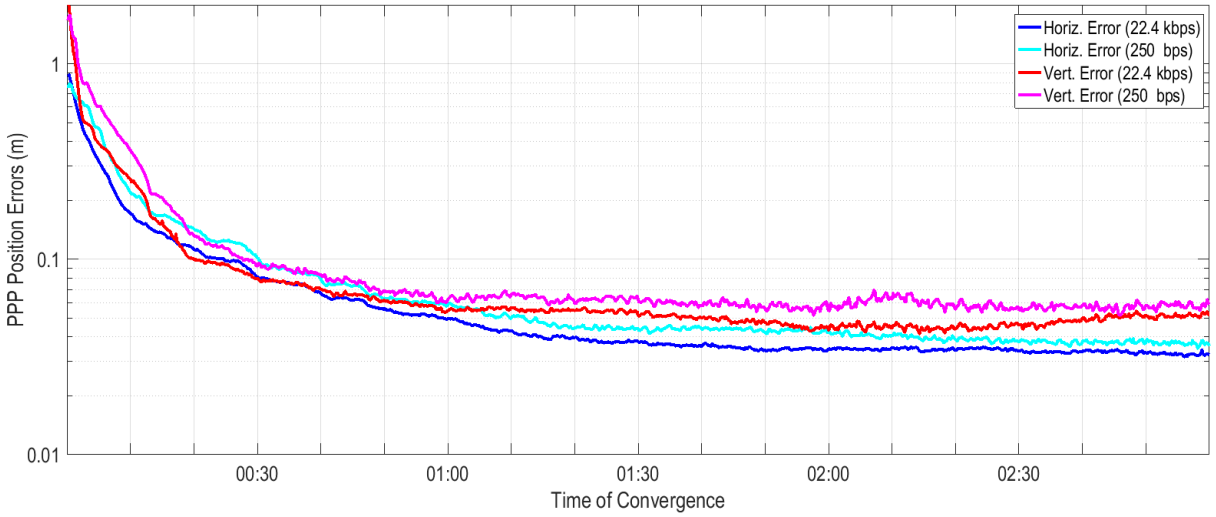

Figure 9. RMSE of horizontal (blue) and vertical (red) errors using RTCM (dark) and recovered (light) messages. PPP solutions calculated using MDC1F between Sep. 2nd and Sep. 21st 2017

The two solutions shown in Figure 9 are comparable, with differences between RMSs never exceeding 2cm after convergence. In contrast to Figure 7 however, the difference between accuracy can be more clearly seen in this case. This is because the differences stem from real-valued ambiguities and not from resolved ambiguities.

	MADOCA direct	MADOCA recovered
Horizontal accuracy <10cm	24 min 50 sec	27 min 00 sec
Vertical accuracy <10cm	18 min 50 sec	26min 50 sec
Horizontal accuracy after 1 hour	3.64cm	4.28cm
Vertical accuracy after 1 hour	4.95cm	5.98cm

Table 7. PPP performance using direct and recovered messages

Compared to the PPP results from CLK93 the horizontal errors are larger, with a 12 % increase in steady state accuracy and a 4-5 minute increase in convergence time (to below 10cm). However vertical errors seem smaller, with a 30% reduction in steady state accuracy and 7 to 10 minute longer convergence times. The degradation of horizontal accuracy for recovered messages is about 17% of steady state accuracy and about 2 minutes of convergence time. The degradation of accuracy in vertical is more significant, with 20% increase in steady state errors and a 10 minute longer convergence time. For all four solutions, the results obtained using recovered or original products were comparable. The degradation of accuracy was statistically detectable both as steady state accuracy and in terms of convergence times. However both can boast a 5cm accuracy on horizontal position and 10 cm accuracy in vertical positioning..

5. SUMMARY

The research presented in this paper studied the feasibility of transmitting corrections for multi-GNSS, high accuracy Precise Point Positioning using a 250 bps (212 bps equivalent) data rate channel. Products for dual-frequency, ambiguity-resolved PPP were generated from existing real-time PPP streams: JAXA's MADOCA and CNES's PPP-Wizard based streams. MADOCA stream was a GPS+GLONASS+QZSS product with a 1 second update rate, PPP-Wizard was a GPS+GLONASS+Galileo+BeiDou stream with 5 second update rate.

Compact messages were designed with a 2 minute update rate for orbit and signal biases, and a flexible update scheme for clock corrections designed to keep extra errors below 1cm. Using this encoding method, a 250 bps channel could support about 102 satellites for MADOCA type corrections and 126 satellites for PPP-Wizard type corrections.

Alhough the message compaction did lead to some performance degradation in PPP solutions the difference in RMS errors was below 1cm for both vertical and horizontal position components, and all types of solutions achieved better than 5cm horizontal and 10cm vertical RMS accuracy. Differences in convergence time to within 10cm were about 2-3 minutes longer with recovered messages, equivalent to less than 16%. Differences in convergence time were more significant for vertical positioning, reaching 30% for both streams.

ACKNOWLEDGEMENTS

This research is funded through the Australian Cooperative Research Centre for Spatial Information and is performed as part of the CRCSI project 1.22. The CRCSI research consortium consists of Geoscience Australia, Land Information New Zealand, RMIT University, Victoria Department of Environment, Land, Water & planning, Position Partners Pty. Ltd. and Fugro Satellite Positioning Pty. Ltd.. The authors would also like to thank JAXA for maintaining the MADOCA products and the CNES for maintaining the CLK93 real-time stream.

REFERENCES

Aubault-Roudier M., Laurichesse D., Bitar H. Al, Raimondi M., Lesage P., Sfeir A., Klein M., Sihrener M., Ramponi N. (2016), "Demonstration: E5b Signal Containing Value-Added Information Broadcast in Real Time via the SES ASTRA 5B GEO Satellite," Proceedings of the 29th International Technical Meeting of The Satellite Division of the Institute of Navigation (ION GNSS+ 2016), Portland, Oregon, pp. 3355-3364.

Banville S., Collins P., Zhang W., and Richard B. Langley (2014), "Global and Regional Ionospheric Corrections for Faster PPP Convergence," NAVIGATION, Journal of the Institute of Navigation, vol. 61, pp. 115-124.

Chang, X. W., Yang X., Zhou T. (2009), "MLAMBDA: a modified LAMBDA method for integer least-squares estimation", Journal of Geodesy, Vol. 79, 9, 2005, p 552-565

Fernandez Hernandez I., Rodriguez I., Tobias G., Calle J. D., Carbonell E., Seco-Granados G. Simon J, Blasi R. (2015), "Galileo Commercial Service - Testing GNSS High Accuracy and Authentication", Inside GNSS, Vol 10,1.

Ge M., Gendt G., Rothacher M., Shi C., Lui J., (2007), "Resolution of GPS carrier-phase ambiguities in Precise Point Positioning (PPP) with daily observations," Journal of Geodesy, vol. 82, pp. 389–399, 2007.

IGS, (2015). "Real-time Service", http://rts.igs.org/, Accessed September 2015.

Japan Aerospace Exploration Agency, (2017). Interface Specification for MADOCA-SEAD revision A. https://ssl.tksc.jaxa.jp/madoca/public/doc/Interface_Specification_A_en.pdf

Juan J. M., Hernandez-Pajares M., Sanz J., Ramos-Bosch P., Aragon-Angel A., Orus R., et al. (2012), "Enhanced Precise Point Positioning for GNSS Users," IEEE Transactions on Geoscience and Remote Sensing, vol. 50, pp. 4213-4222.

Kouba, J., (2009), "A Guide to using International GNSS Service (IGS) Products", http://igscb.jpl.nasa.gov/components/usage.html, Accessed October 2016.

Laurichesse D., Mercier F., Berthias J., Broca P., Cerri L., (2009), "Integer Ambiguity Resolution on Undifferenced GPS Phase Measurements and Its Application to PPP and Satellite Precise Orbit Determination," NAVIGATION: Journal of The Institute of Navigation, vol. 56, pp. 135 - 149.

Li, X., Ge, M., Dousa, J., Wickert, J. (2014): Real-time precise point positioning regional augmentation for large GPS reference networks. - GPS Solutions, vol 18 , 1, p. 61-71.

Prange, L., Orliac, E., Dach, R. et al. (2017), "CODE's five-system orbit and clock solution—the challenges of multi-GNSS data analysis", Journal of Geodesy, Vol. 91, 4, pp. 345-360

Rovira-Garcia A., Juan J. M., Sanz J., and González-Casado G. (2015), "A Worldwide Ionospheric Model for Fast Precise Point Positioning," IEEE Transactions on Geoscience and Remote Sensing, vol. 53, pp. 4596-4604.

Takasu, T., A. Yasuda (2009) "Development of the low-cost RTK-GPS receiver with an open source program package RTKLIB" International Symposium on GPS/GNSS pp 4-6

Teunissen, P. J. G. and Khodabandeh A.(2015). "Review and principles of PPP-RTK methods." Journal of Geodesy 89(3) pp 217-240

Trimble. (2017). Trimble CenterPoint RTX. Available: http://www.trimble.com/Positioning-Services/CenterPoint-RTX.aspx

Zhang, H., Gao Z. Ge M., et. al. (2013), "On the Convergence of Ionospheric Constrained Precise Point Positioning (IC-PPP) Based on Undifferential Uncombined Raw GNSS Observations". Sensors 2013, vol 13, pp:15708-15725

Zumberge, J. F., Heflin M. B., Jefferson D.C., Watkins M. M. Webb F. H., (1997). "Precise Point Positioning for The Efficient and Robust Analysis of GPS Data from Large Networks", Journal of Geophysical Research, 102, B3, 5005-17.